How Good is a Paleoseismic Record of Megathrust Earthquakes for Probabilistic Forecasting?

Francisco Acuña[1], Gonzalo A. Montalva*[1], and Daniel Melnick[2]

Abstract

Time-dependent earthquake forecast depends on the frequency and number of past events and time since the last event. Unfortunately, only a few past events are historically documented along subduction zones where forecasting relies mostly on paleoseismic catalogs. We address the role of dating uncertainty and completeness of paleoseismic catalogs on probabilistic estimates of forthcoming earthquakes using a 3.6-ka-long catalog including 11 paleoseismic and 1 historic ($M_w \geq 8.6$) earthquakes that preceded the great 1960 Chile earthquake. We set the clock to 1940 and estimate the conditional probability of a future event using five different recurrence models. We find that the Weibull model predicts the highest forecasting probabilities of 44% and 72% in the next 50 and 100 yr, respectively. Uncertainties in earthquake chronologies due to missing events and dating uncertainties may produce changes in forecast probabilities of up to 50%. Our study provides a framework to use paleoseismic records in seismic hazard assessments including epistemic uncertainties.

Cite this article as Acuña, F., G. A. Montalva, and D. Melnick (2021). How Good is a Paleoseismic Record of Megathrust Earthquakes for Probabilistic Forecasting? *Seismol. Res. Lett.* **XX**, 1–10, doi: 10.1785/0220210044.

Supplemental Material

Introduction

In subduction zones, the average recurrence interval of great tsunamigenic earthquakes is commonly larger than the length of instrumental data and historical chronicles, and thus paleoseismic catalogs of past seismic events are valuable records for the probabilistic forecasting of an imminent forthcoming earthquake and assessment of the associated hazards. It has been long recognized that time-dependent models perform much better than time-independent (i.e., Poisson) models for the predictive assessment of seismic hazards associated with individual geologic faults (Bufe *et al.*, 1977). Pioneers in describing the time of recurrence between events from temporal models were Rikitake (1974) using a Gaussian distribution and Hagiwara (1974) using Lognormal, Gamma, and Weibull distributions. Subsequently, Nishenko and Buland (1987) first combined historical and geological records of largest earthquakes in the Pacific region (plate boundaries or along specific faults) and observed that the times between events fit Weibull distributions better than Gaussian. These authors also introduced the use of the Lognormal distribution, which since has become common practice for several applications in seismology (e.g., Convertito and Faenza, 2014) and one of the most relevant for computing earthquake probabilities in California (WGCEP 2007 and previous works). Subsequently, Matthews *et al.* (2002) proposed the Brownian passage time (BPT) model as an application of the inverse Gaussian distribution that is more consistent with the elastic rebound theory, and Zöller (2018) showed that BPT models are adequate for assimilating paleoseismic events and instrumentally recorded earthquakes of different magnitudes and duly reproduce recurrence intervals of great earthquakes. However, for time intervals relevant to engineering projects the Gutenberg–Richter relation fails to describe the distribution of magnitudes, including great earthquakes, along large subduction megathrust faults, emphasizing the need to study different recurrence models tailored for the use of paleoseismic records.

Subduction earthquake paleoseismology is different from crustal earthquake paleoseismology, because it relies on proxies for regional deformation and shaking, as opposed to directly sampling the fault zone. These proxies include estimates of coastal land-level change, tsunami inundation, and/or ground shaking (such as turbidites and lacustrine deposits), and their spatial and temporal information is used to define past rupture limits and recurrence intervals (Garrett *et al.*, 2016; Clark *et al.*, 2019; Moernaut, 2020; Walton and Staisch *et al.*, 2021). Here, we analyze the predictive potential of a 3.6-ka-long paleoseismic record at the Valdivia segment of the Chilean subduction zone to predict the most recent earthquake, which occurred in

1. Departamento de Ingeniería Civil, Universidad de Concepción, Concepción, Chile, https://orcid.org/0000-0001-8598-7120 (GAM); 2. Instituto de Ciencias de la Tierra, TAQUACH, Universidad Austral de Chile, Valdivia, Chile, https://orcid.org/0000-0001-8397-7391 (DM)

*Corresponding author: gmontalva@udec.cl

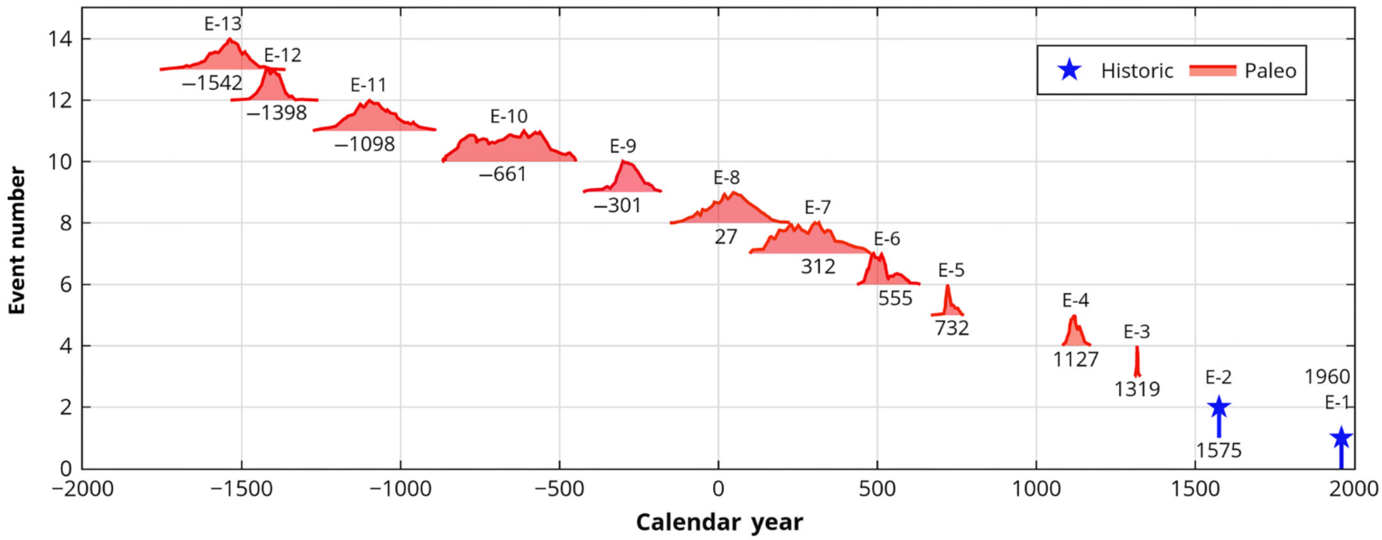

Figure 1. Paleoseismic and historic events in the Calafquen Lake (CAL) record (Moernaut *et al.*, 2018). Bold-red lines denote probability density functions (PDFs) given by radiocarbon dating uncertainties of E-5 to E-13 paleoearthquakes, and by varve counting (technique that allows precise dating of paleoseismic sedimentary features, based on the counting of thin layers of annually deposited sediments) for E-3 and E-4. Blue lines and stars show the timing of the historical events E-1 and E-2. The color version of this figure is available only in the electronic edition.

1960 (M_w 9.5). We test different recurrence models and simulate the effect of catalog completeness as well as of dating uncertainties on the resulting probabilistic predictions. Our results have implications for the use of paleoseismic catalogs in the assessment of seismic hazards along subduction zones.

Methods

Paleoseismic record

The historic and paleoseismic records from south–central Chile show that megathrust events similar to the 1960 and 1575 events occurred on average every 292 ± 93 yr over the past 2 ka (Lomnitz, 1970; Cisternas *et al.*, 2005). Moernaut *et al.* (2018) analyzed lacustrine sediments from Calafquen Lake (CAL) using turbidite paleoseismology. These turbidite records in lake sediments can form such high-quality "natural seismographs" (Strasser *et al.*, 2013; Doughty *et al.*, 2014), which record strong seismic shaking as specific deposits or deformation structures within the lacustrine sedimentary infill (for details on how these records are developed see Moernaut, 2020). Moernaut *et al.* (2018) analyzed the cores using sedimentological analysis and high-resolution magnetic susceptibility measurements, and estimated probability distributions of earthquake dates using radiocarbon and varve-counting techniques (further details in Moernaut *et al.*, 2014, 2018). The CAL record (Moernaut *et al.*, 2018) includes 13 megathrust events (see Fig. 1 and Table S1), 11 paleoseismic, and 2 historic earthquakes covering 3.6 ka. The catalog has been cross validated by independent records obtained from other lake basins as well as along the coast (Cisternas *et al.*, 2005; Kempf *et al.*, 2017) and is assumed to be complete for $M_w > 8.6$ earthquakes.

Database treatment

Unlike historical or instrumental records, in which the date of an event is known with precision, paleoseismic records compose an uncertainty on the occurrence date of a given event that conditions any subsequent calculations. For the CAL record, the actual event age probability density function (PDF) of each event was obtained from Moernaut *et al.* (2018). The fitting parameters of time-dependent recurrence models were estimated using the approach of Biasi *et al.* (2015), based on the generation of likelihood surfaces from sequences of events drawn from each age PDFs independently, which allows the quantification of recurrence parameters and their uncertainties. This methodology seeks to preserve the structure of the dating obtained from radiocarbon techniques, considering its uncertainty. The generation of these series could allow events to overlap, for example, that in a generated series E-7 happen after E-8 because the dates were drawn from each PDF, which would be wrong. This would also imply, for a small number of cases, negative recurrence intervals. Because of the stratigraphic superposition criteria, we know that, in fact, the sedimentary deposit (turbidite) associated with E-7 was deposited above that of E-8 and therefore must be younger. To avoid this problem, we forced the recurrence intervals to be positive, hence preserving the chronologic order, and applied a geological restriction to account for the minimum time between events that was required to accumulate the amount of background lacustrine sediment deposited between turbidites samples. An analysis of several lakes in the region suggests that background sedimentation rates in the central part of the lacustrine basins, which occurs by suspension settling, have a mean of 1 ± 0.1 mm/yr (Moernaut, 2020).

Therefore, we assume a minimum inter-event time of 50 yr for this study, which should be considered a conservative estimate because ~100 mm is the minimum thickness of lacustrine sediments separating each turbidite in the CAL record (Moernaut *et al.*, 2014).

Earthquake recurrence models and parameter fitting

Time-dependent models applied to earthquake recurrence studies have been commonly used in several regions around the world, such as by Pasari and Dikshit (2014, 2015) and Pasari (2019) in India, and Kulkarni *et al.* (2013) in the Cascadia subduction zone. Biasi *et al.* (2015) concluded at the Alpine fault (New Zealand) that time-dependent models offer a better characterization of the seismic recurrence from a given source than an exponential model. As shown by Biasi *et al.* (2015), a "best" model to assess the temporal recurrence of earthquakes has not been yet proposed. We use four time-dependent (Lognormal, BPT, Weibull, and Gamma) models and one time-independent (exponential) model to study their capacity to forecast the 1960 earthquake using the CAL record. See Table S2 in the supplemental material for density functions and parameter details of these models.

In time-dependent recurrence models based on paleoseismic data, the forecast of a new event is influenced by the quality and quantity of events in the record. In paleoseismic records, the sample size for uncertainty estimation is limited to the number of earthquakes, which is usually small, and it controls the resolution of the fitting parameters. Ellsworth *et al.* (1999) used a bootstrap technique in a record for the San Andreas fault in California to obtain a wider range of recurrence parameters that could generate the observed set of events; they concluded, however, that recurrence rates cannot be estimated with adequate confidence for records containing fewer than 10 events.

Because the dating of paleoseismic records is not exact, we adopted the modification to the maximum-likelihood method proposed by Biasi *et al.* (2015). In a relatively regular event record, the likelihood reaches a peak near the parameters that best describe the series. In contrast, for a series that consists only of a few events, which are less regular or that have wide dating uncertainties, the likelihood will be less defined, and a wider range of parameters may be generated from such a series (Biasi *et al.*, 2015). The likelihood surface is constructed by evaluating equation 1, on a grid of points $\theta ij = (\theta 1j, \theta 2k)$, covering the required confidence level, and the height of the surface is proportional to the likelihood of observing the data within the paleoseismic series for this pair of parameters.

$$L(M,T) = \prod_{i}^{\mathrm{Nev}-1} P(T_i|M,\theta), \tag{1}$$

in which L: likelihood function, M: temporal model, T: random variable (time between events), θ_{ML}: maximum-likelihood parameters, and Nev: event number.

We generate series with 600 sets of interevent times between events from the dating distributions (600 sequences or sets of times between events) and analyze a parameter grid space containing the required uncertainty. For each pair of parameters, we calculate the likelihood of each of the interevent time sets assigning the average of the obtained likelihood. The most likely recurrence parameters given the event series were defined as the peak of the likelihood surface. The 95% confidence intervals for the recurrence parameters are defined using the likelihood ratio method; a contour in the likelihood surface (Fig. S1) defines different confidence intervals. This method assumes an asymptotic Chi-square distribution for the difference between the log likelihood of the maximum-likelihood parameters and the grid combinations (Biasi *et al.*, 2015). For $\mathrm{Log}(\frac{L(\theta_{\mathrm{ML}}|M,T)}{L(\theta|M,T)})$ below 2.995 (i.e., if equation 2 holds), the estimated parameters are with 95% confidence correct.

$$\mathrm{Log}\left(\frac{L(\theta_{\mathrm{ML}}|M,T)}{L(\theta|M,T)}\right) = l(M,T) - l(\theta|M,T) < 2.995, \tag{2}$$

in which L: likelihood function, l: log likelihood, M: temporal model, T: random variable (time between events), and θ_{ML}: maximum-likelihood parameters.

An important technical advantage in the estimation of recurrence parameters is the incorporation of open intervals, which becomes important when the time between the last event and the present day (T_{MRE}) approaches the average recurrence time (Ellsworth *et al.*, 1999). Biasi *et al.* (2015) include the open interval by modifying the likelihood estimate with the following expression:

$$L(\theta; M, T, T_{\mathrm{MRE}}) = L(\theta; M, T) * [1 - CDF(T_{\mathrm{MRE}}; M, \theta)]. \tag{3}$$

We used the CAL record (Moernaut *et al.*, 2018) to study the influence that event age PDF has on the model parameters to forecast a forthcoming megathrust event. We also used the CAL record to forecast the occurrence of a future event in the next 50–100 yr considering closed intervals that is the probability of one event occurring in these intervals.

Results

Forecasting the 1960 Chile earthquake

The first historical earthquake in the CAL record occurred in 1575 and thus 385 yr elapsed to the last event in 1960. In a practical exercise to determine the utility of the CAL record for forecasting future events, we predicted the occurrence of the last megathrust event of the series (E-1, 1960, M_w 9.5), from the information of the 12 remaining events. We calculated the recurrence parameters by arbitrarily setting the clock to the year 1940, hence for an open interval of 365 yr (see Table S3 and Fig. 2a), with occurrence forecasts for the next 50 and 100 yr. Time-dependent models can predict the probability of occurrence

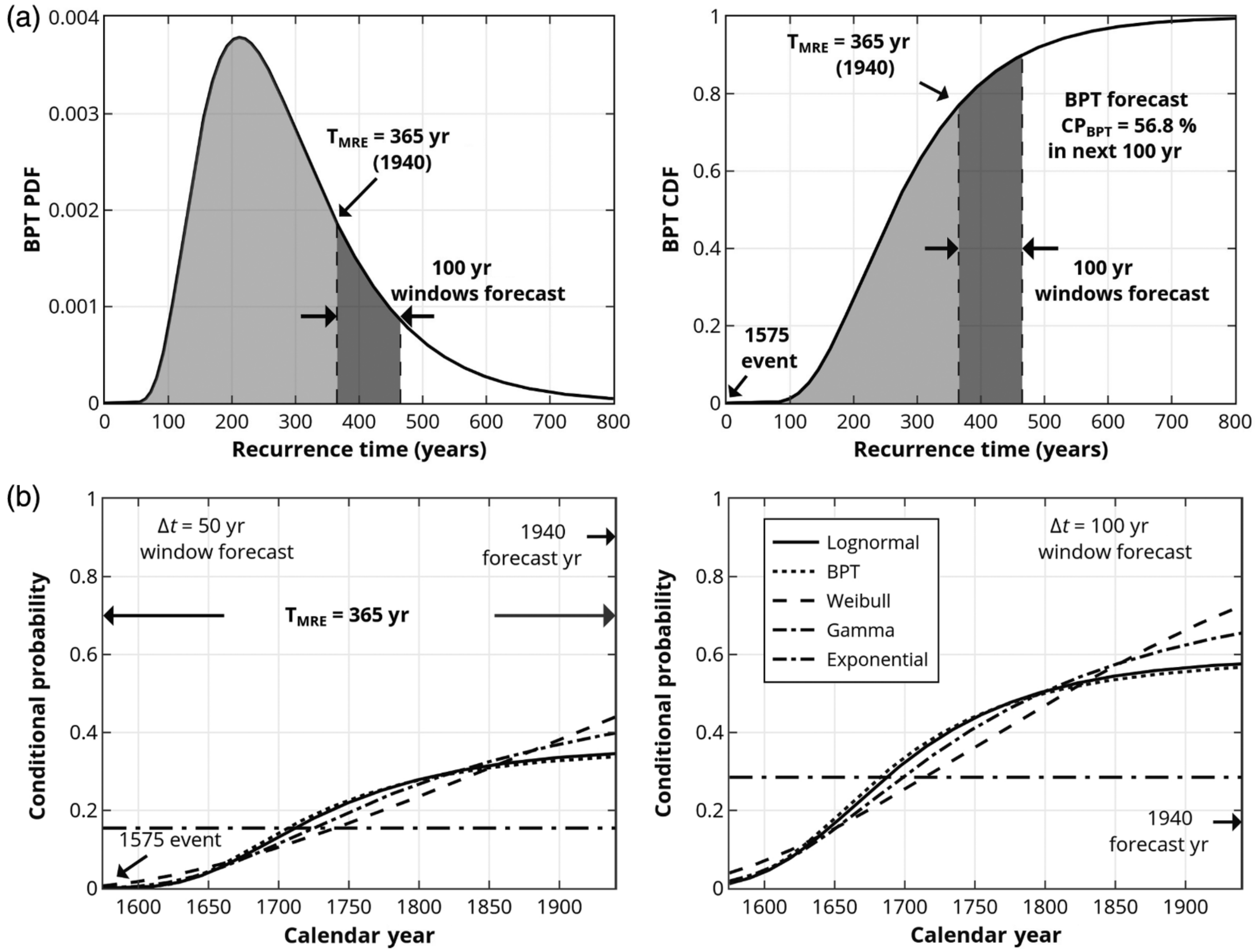

Figure 2. Forecasting probability results. (a) Brownian passage time (BPT) model, PDF, and cumulative distribution function (CDF) for an open interval of 365 yr (1575–1940) considering a forecasting window of 100 yr. The ratio between gray and light gray values in the CDF allows obtaining the conditional probability (CP) of occurrence (56.8%). (b) Occurrence forecast of the 1960 earthquake with a 365 yr open interval using the CAL record (Moernaut *et al.*, 2018).

of the 1960 event to between 34% and 44% within 50 yr, and 57% and 73% for the next 100 yr (see Table S4 for details).

Figure 2b compares the conditional probability (CP) curves for forecasts of 50 and 100 yr for the five recurrence models, observing that the Weibull model generates the highest probability of rupture in both cases. The exponential distribution (time-independent) generates forecasts on the order of 50% lower than the time-dependent models after a long open interval has been observed (the case of forecasting the 1960 great earthquake).

We evaluate the influence of the actual event age PDF, considering it as normal or uniformly distributed. This effect immediately generates an increase in uncertainty, because wider time intervals between events are generated, which influence the parameter estimates.

For example, for a Lognormal model (normal dating) we obtain $(\mu, \sigma) = (5.58, 0.49)$, and for the uniform case $(\mu, \sigma) = (5.57, 0.51)$; the increase in the standard deviation with respect to the PDF dating (see Table S3) generates a decrease in the 1960 event forecast on the order of 5% and 10% for 50 and 100 yr windows, respectively. Figure 3 shows the decrease in CP obtained by disregarding the age PDF for BPT and Weibull models, which yield results very similar to Lognormal and Gamma models.

Testing the integrity of the CAL record

From the previous results, we analyze the robustness of the forecast of the 1960 event, exploring the impact that an event might have been missed from the record. For this purpose, we analyze the results obtained by means of the permutation generated when an event is eliminated. Figure 4 shows the results obtained in the permutation analysis considering the BPT and Weibull models.

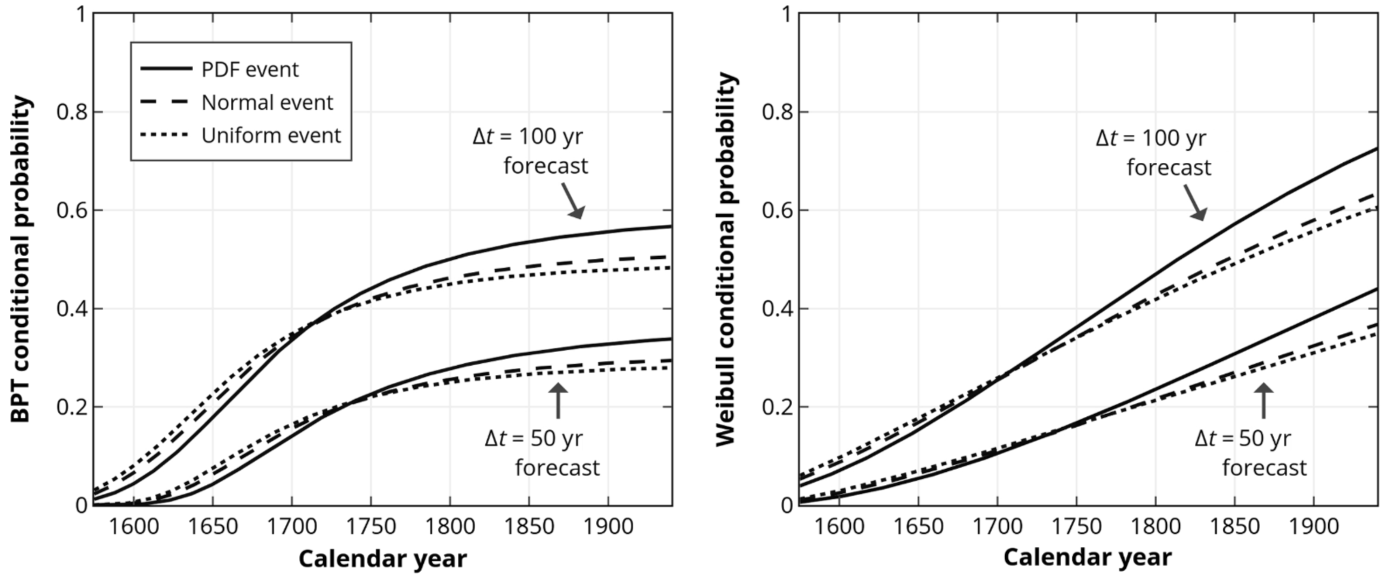

Figure 3. Effect of modeling dating uncertainty using normal, uniform, and PDFs of event ages in the 1960 earthquake forecast for 50 and 100 yr windows considering time-dependent Weibull and BPT models. The difference is more noticeable in the Weibull model with 10% in 50 yr and 12% in 100 yr.

For a BPT model, we observe that the 1960 forecast would be influenced by the absence of an event (or because the event was lost from the sedimentary record by erosion or any other processes and not recognized as such in the interpretation). There is a 29% decrease of mean CP within the next 100 yr when event E-10 (−661) is removed, whose time of recurrence with respect to the next event (E-11, −1098) is 437 yr (the longest interval in the series). On the contrary, the forecast increases up to 4% when removing the last event of the series (E-13, −1542), which has an average recurrence time of 144 yr with respect to the following event (the lowest recurrence time in the series). Removing an event in the CAL record has a significant effect on the stability of the forecast of the 1960 earthquake. This suggests the need to increase redundancy in the evidence to avoid missing events for which it is essential to strengthen paleoseismological research.

We test the effect of dating uncertainties by assuming that ages follow normal distributions and by decreasing the standard deviation of these distributions by 10%–80%, simulating therefore greater precision in the dating of each event. We evaluate the effect of this continuous simulated reduction in uncertainty on the 1960 forecast using the BPT and Weibull models (Fig. 5). The results show a significant improvement in the forecast, strongly suggesting that greater precision in dating techniques corresponds to a first order factor within the temporal recurrence analysis. For example, searching for records that have annually deposited varves and making the effort of counting them could improve the age dating resolution. We also randomly seeded an extra event into the CAL catalog to assess how it influences the forecasts (Fig. 6). The highest impact occurs when the introduced "missed event" is located between events E-10 and E-11, resulting in an increase of the 1960 earthquake forecast to 62% and 83% for BPT and Weibull distributions, respectively.

Forecasting the next 50–100 yr

We analyze the occurrence of an event within the next 50 and 100 yr for the five recurrence models. Slight differences are observed in the parameter calculations when varying the treatment method for dating uncertainties (Table S5), which can be directly observed by means of the likelihood surfaces (Fig. S1). We observe an increase in the standard deviation and its confidence intervals for the normal and uniform distribution cases (Fig. S2). The actual event PDFs generate narrower recurrence intervals and standard deviations than normal and uniform distributions; this may be due to the skewness of some of the PDFs, which the normal and uniform distributions fail to capture. The CP of a megathrust event for the next 50 yr is quite low (<3.5% for PDF time-dependent models). For the next 100 yr, temporal models forecast an up to 11% probability of occurrence, whereas the exponential model forecast a significantly higher probability of occurrence (see Table S6). The different treatment of uncertainty generates slight differences of up to 4% for 100 yr forecasts, whereas within 50 yr these are negligible. In all cases, the exponential model tends to overestimate the occurrence of a new event, relative to time-dependent models. Matthews *et al.* (2002) and Pasari (2019) found that at the beginning of the seismic cycle the forecasts obtained in Lognormal and BPT models are low, whereas in time windows higher than one-fourth of the average recurrence, they begin to increase significantly. This difference is seen in the 50 and 100 yr forecasts for CAL record (Moernaut *et al.*, 2018) as well (Fig. 2b).

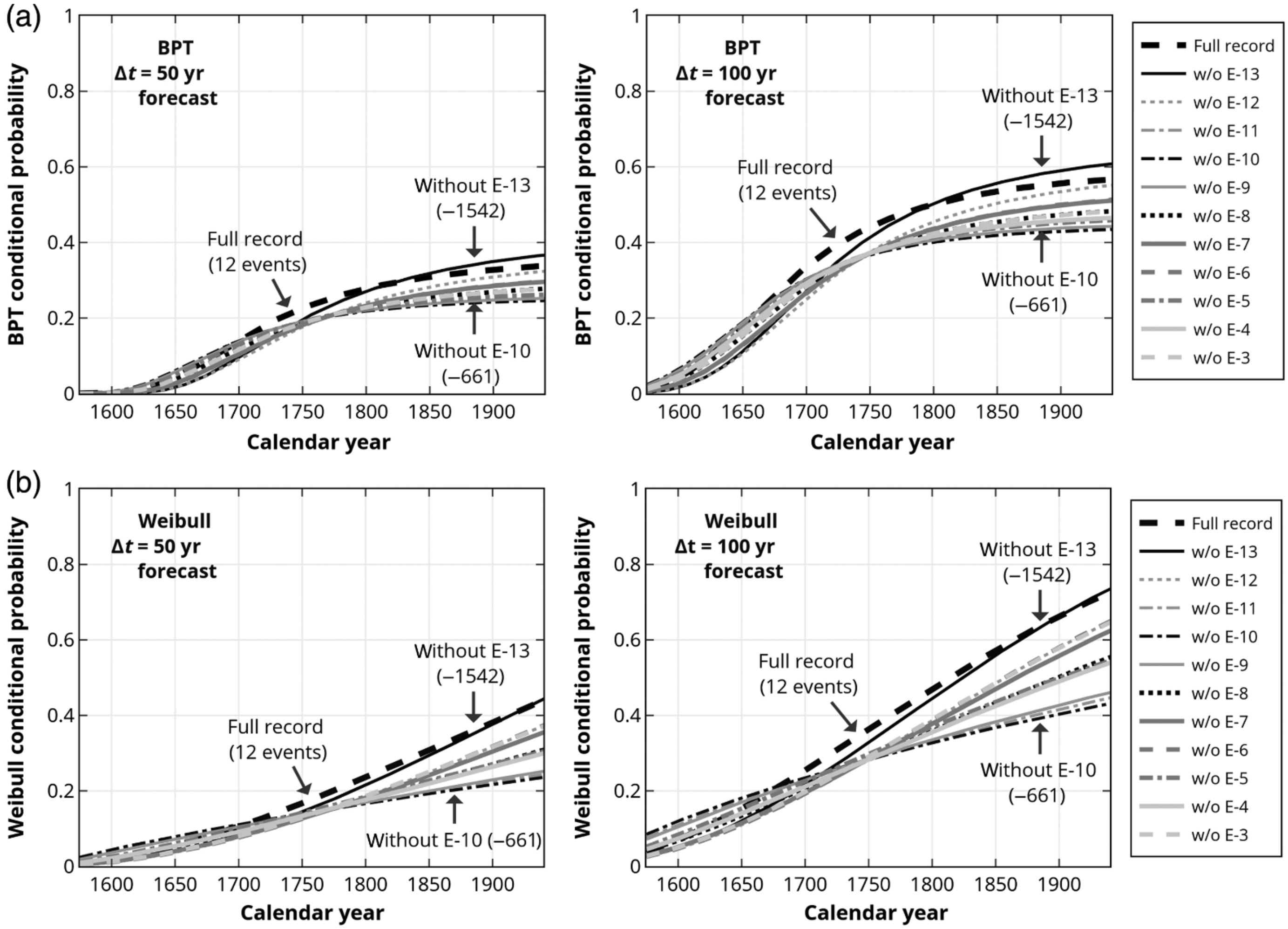

Figure 4. Simulations to quantify the role of a missing or unrecognized event in the sedimentary record of prehistoric earthquakes in the CAL Record (Moernaut *et al.*, 2018) on the 1960 earthquake forecast. Results for the (a) BPT and (b) Weibull models are shown. (w/o: without event). Dashed lines show the forecast using the CAL record for 50 and 100 yr windows. In both cases, the forecast decreases (up to 29% in mean CP over 100 yr with the Weibull model) by removing event E-10 and slightly increases by removing event E-13 (see Table S1 for further details of event dating).

Discussion and Conclusions

All four time-dependent models forecast the occurrence of the 1960 earthquake much better than a simpler, one-parameter memoryless model such as the exponential model. The latter underestimates the probability of occurrence by at least 50%, relative to time-dependent models, which implies that using an exponential model forecasts the 1960 earthquake with a lower likelihood. The opposite is found when computing the probability of an earthquake ($M_w > 8.6$) within 50 or 100 yr from now in the same region, for which the exponential model overpredicts the probability by at least 360% and 60%, respectively, relative to time-dependent models (Table S6).

The use of actual event age PDFs for each event results in a 10% higher mean forecast probability of the 1960 event, compared to uniform or normal distributions (Fig. 3). The statistical distribution used to model the paleoseismic record (i.e., all 12 events prior to 1960) varies more significantly when T_{MRE} is close or greater than the mean recurrence interval (Fig. 2b). BPT and Lognormal models as well as Weibull and Gamma models have a similar response to the variation of the T_{MRE}, each pair producing similar forecasts. When attempting to capture the associated epistemic uncertainties for seismic hazard assessments, we recommend using at least a pair of models (e.g., BPT and Weibull), as much of the difference between the shape of the four renewal models considered in this study is in the shape of their tails.

Williams *et al.* (2019), Griffin *et al.* (2020), and Moernaut (2020) showed that quasi-periodic ruptures are likely the norm for large, regularly occurring earthquakes, which is consistent with our results. If the processes associated with interseismic accumulation of energy between great earthquakes were similar between any pair of events (e.g., Melnick *et al.*, 2017), either historical or prehistoric, the predictive capacity of a limited series would be very high (Rhoades and van Dissen, 2003). However, this is not the case due to the complex mechanisms

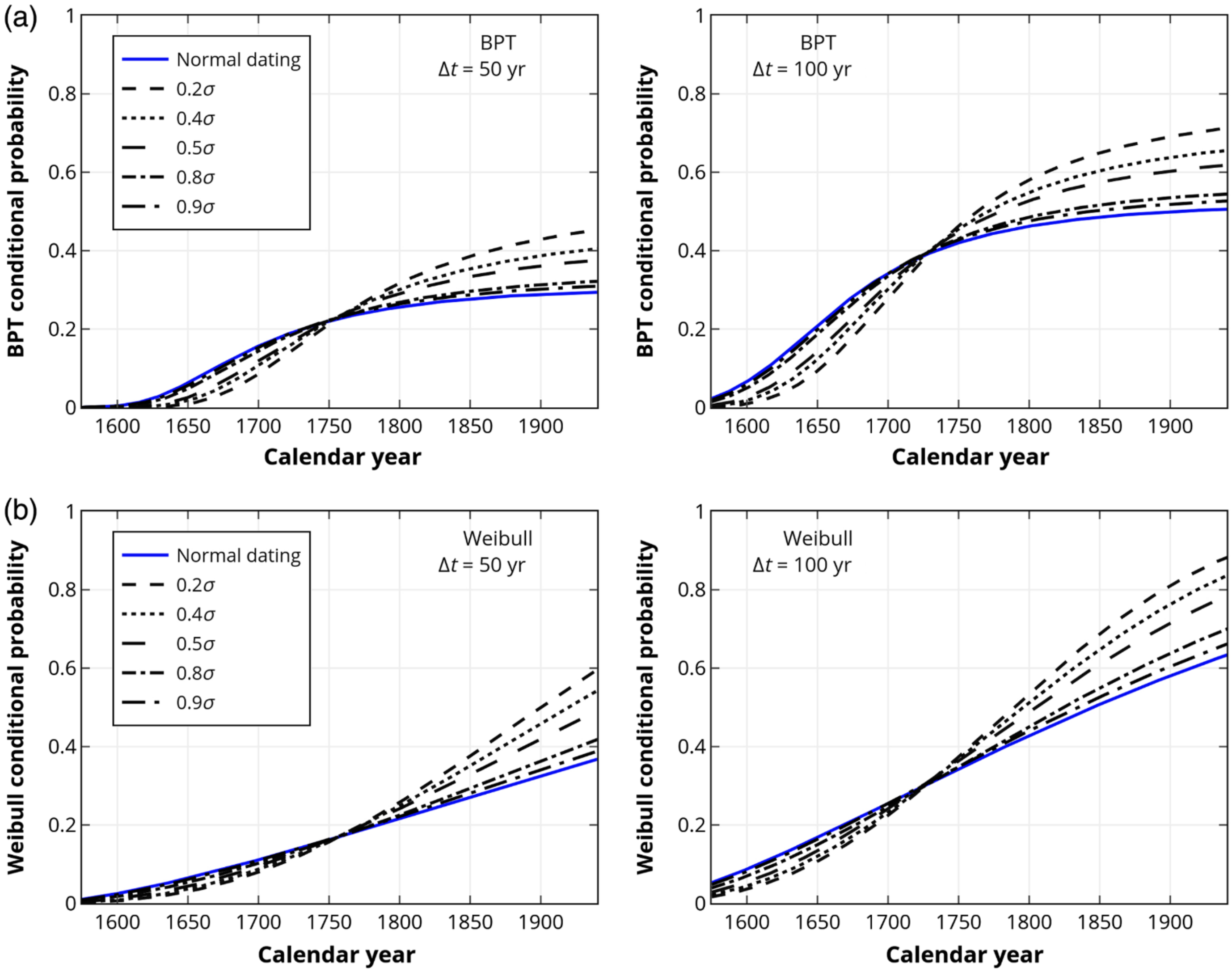

Figure 5. Simulations to assess the role of reducing dating uncertainties of the paleoseismic record in the 1960 earthquake forecast. Blue lines show forecast using the reported dating uncertainties; stippled and dotted lines show the reduction in uncertainties as a function of standard deviation (σ). The simulations include: (a) BPT and (b) Weibull models, and consider that the actual event age PDF is normally distributed and σ reductions of 10%–80% (0.9–0.2 σ). The reduction in σ causes an important improvement in the 1960 forecast. The color version of this figure is available only in the electronic edition.

involved in the seismic cycle along subduction zones. Between the 1575 and 1960 earthquakes, two relatively large events occurred within the Valdivia segment in 1737 and 1837; however, these events are not in the CAL series (Moernaut *et al.*, 2018) because they were significantly smaller in magnitude and rupture area than both the 1575 and 1960 earthquakes (Cisternas *et al.*, 2005, 2018). Lomnitz (2004) estimated magnitudes of 7.8 and 8 for the 1737 and 1837 events, respectively, and a reanalysis of historical documents and geologic evidence suggests they ruptured only limited portions of the northern and southern portions of the 1960 rupture (Cisternas *et al.*, 2017). However, these events likely played a role in the larger-than-average duration of the interseismic period between the 1575 and 1960 earthquakes, a role that is not considered in the assumption made when using time-dependent models. The duration of the interseismic period may be controlled by interactions between earthquakes rupturing at different depths in the subduction fault, as suggested by a modeling study comparing recurrence times between the 1960 and 2016 M_w 7.6 earthquakes in Chile (Moreno *et al.*, 2018) as well as among other smaller localized historical ruptures along several subduction zones (Philibosian and Meltzner, 2020).

Another factor that affects the interval between great earthquakes is the interaction between segments, as suggested by an analysis of the changes in surface velocities estimated using Global Positioning System after the 2010 M_w 8.8 earthquake that affected the region immediately north of the 1960 rupture zone (Melnick *et al.*, 2017). A positive increase in surface velocities, interpreted as the result of a higher degree of interseismic

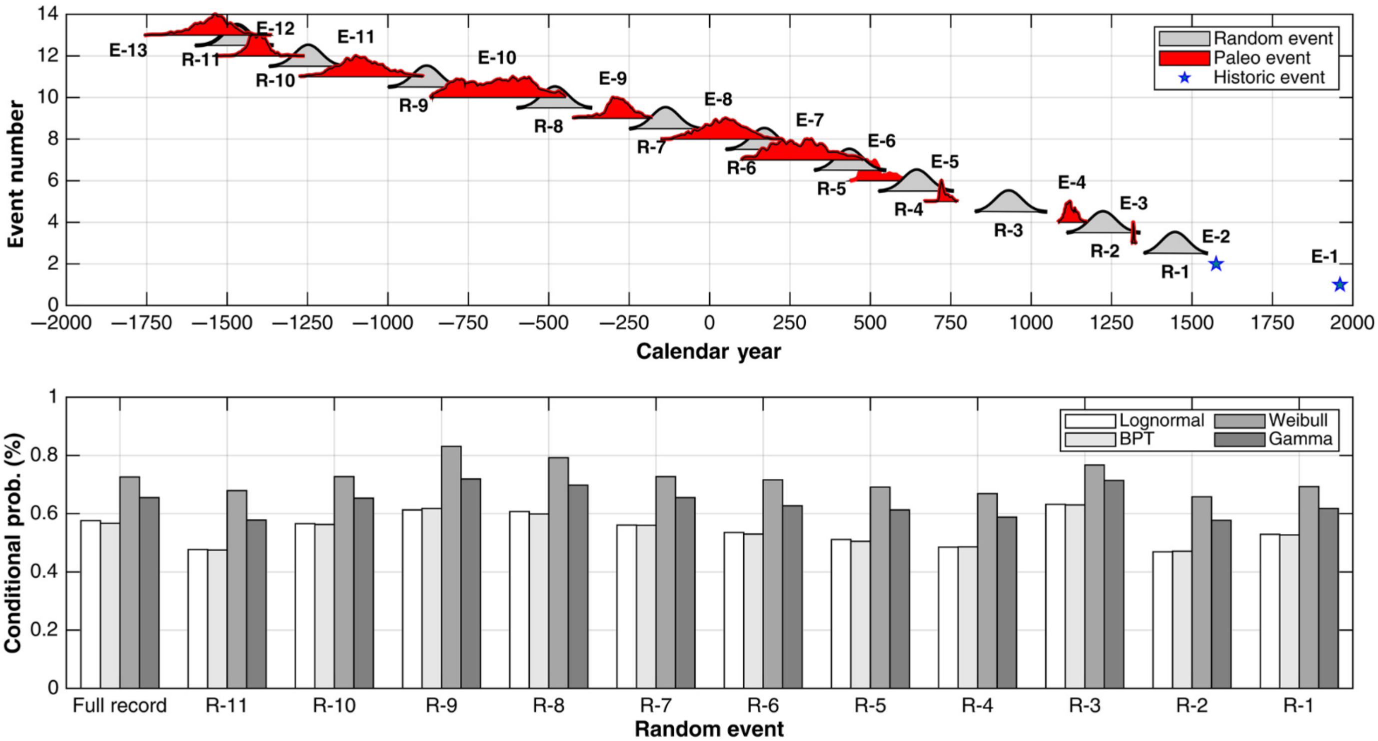

Figure 6. Influence on the 1960 forecast for time-dependent models, when a normally distributed random event (R-1 to R-11) is seeded between each of the dated events (E-1 to E-13). The greatest impact on forecast occurs when considering the R-9 (between E-10 and E-11) and R-8 (between E-9 and E-10) events. The color version of this figure is available only in the electronic edition.

plate locking, was observed after the 2010 earthquake in the regions affected by the 2015 M_w 8.3 Illapel and 2016 M_w 7.6 Melinka earthquakes. The latter was located within the 1960 rupture zone but caused intensities 82% lower than those estimated for the 1960 earthquake and was located at >400 km from the lakes hosting turbidite records; therefore, such smaller events may have been commonly missed in the geologic records. It is plausible that such interactions may have modulated the variable lengths of interseismic periods observed in the CAL record, but more detailed records would be needed to gain further insight on such processes at longer timescales.

The predictive capacity of the tested models to forecast the 1960 event is highly dependent on the number of events and their dating precision in the catalog. A paleoseismic record containing relatively regular events, and more events than the proposed threshold (i.e., <10 events; Ellsworth *et al.*, 1999), would intuitively suggest a reliable predictive potential. This conclusion emphasizes the need for careful and rigorous assessments of the geologic criteria used to construct paleoseismic catalogs, and for the need to use independent sites in cross-validated catalogs (such as lacustrine turbidites, for example). Our results emphasize the need to improve the precision of dating methods, either by using better analytical equipment or by innovating in the use of independent geologic markers, which could lead to an up to 50% increase in predictive capacity. Longer records (>10 events) would allow the identification of clusters, or supercycle behavior, and this cannot be ruled out from short records (e.g., Nelson *et al.*, 2021). We envisage that complementing the renewal models analyzed in our study with physics-based simulations will further help to reduce epistemic uncertainties in earthquake forecasts providing better assessment of seismic hazards.

Data and Resources

The paleoseismic data of the Calafquen Lake (CAL) series were obtained from Moernaut *et al.* (2018). Figures were made using R software (http://www.R-project.org/, last accessed January 2021). Supplemental material includes figures and tables detailing the statistics of each event in the CAL record, the fitting parameters for each model used, along with the epistemic uncertainty associated with the dating of each paleoseismic event (probability density function [PDF], normal, or uniform distributions).

Declaration of Competing Interests

The authors acknowledge there are no conflicts of interest recorded.

Acknowledgments

The authors acknowledge financial support from the Millennium Nucleus CYCLO (The Seismic Cycle Along Subduction Zones) funded by the Millennium Scientific Initiative (ICM) of the Chilean Government Grant NC160025, Chilean Scientific and

Technological Development Support Fund (FONDEF) Grant ID16I20157, Chilean National Fund for Development of Science and Technology (FONDECYT) Grants 1181479 and 1190258, and the ANID PIA Anillo ACT192169.

References

Biasi, G. P., R. M. Langridge, K. R. Berryman, K. J. Clark, and U. A. Cochran (2015). Maximum-likelihood recurrence parameters and conditional probability of a ground-rupturing earthquake on the southern Alpine fault, South Island, New Zealand, *Bull. Seismol. Soc. Am.* **105,** no. 1, 94–106, doi: 10.1785/0120130259.

Bufe, C. G., P. W. Harsh, and R. O. Burford (1977). Steady-state seismic slip—A precise recurrence model, *Geophys. Res. Lett.* **4,** no. 2, 91–94, doi: 10.1029/GL004i002p00091.

Cisternas, M., B. F. Atwater, F. Torrejón, Y. Sawai, G. Machuca, M. Lagos, A. Eipert, C. Youlton, I. Salgado, T. Kamataki, *et al.* (2005). Predecessors of the giant 1960 Chile earthquake, *Nature* **437,** no. 7057, 404–407, doi: 10.1038/nature03943.

Cisternas, M., M. Carvajal, R. Wesson, L. L. Ely, and N. Gorigoitia (2017). Exploring the historical earthquakes preceding the giant 1960 Chile earthquake in a time-dependent seismogenic zone, *Bull. Seismol. Soc. Am.* **107,** no. 6, 2664–2675, doi: 10.1785/0120170103.

Cisternas, M., E. Garrett, R. Wesson, T. Dura, and L. L. Ely (2018). Unusual geologic evidence of coeval seismic shaking and tsunamis shows variability in earthquake size and recurrence in the area of the giant 1960 Chile earthquake, *Mar. Geol.* **396,** 54–66, doi: 10.1016/j.margeo.2018.01.005.

Clark, K., J. Howarth, N. Litchfield, U. Cochran, J. Turnbull, L. Dowling, A. Howell, K. Berryman, and F. Wolfe (2019). Geological evidence for past large earthquakes and tsunamis along the Hikurangi subduction margin, New Zealand, *Mar. Geol.* **412,** 139–172.

Convertito, V., and L. Faenza (2014). Earthquake recurrence, in *Encyclopedia of Earthquake Engineering*, M. Beer, I. A. Kougioumtzoglou, E. Patelli, and I. S.-K. Au (Editors), Springer, Berlin, Heidelberg, 1–21, doi: 10.1007/978-3-642-36197-5_236-1.

Doughty, M., N. Eyles, C. H. Eyles, K. Wallace, and J. I. Boyce (2014). Lake sediments as natural seismographs: earthquake-related deformations (seismites) in central Canadian lakes, *Sediment. Geol.* **313,** 45–67, doi: 10.1016/j.sedgeo.2014.

Ellsworth, W. L., M. V. Matthews, R. M. Nadeau, S. P. Nishenko, P. A. Reasenberg, and R. W. Simpson (1999). A Physically-based earthquake recurrence model for estimation of long-term earthquake probabilities, *U.S. Geol. Surv. Open-File Rept.*, doi: 10.3133/ofr99522.

Garrett, E., O. Fujiwara, P. Garrett, V. M. A. Heyvaert, M. Shishikura, Y. Yokoyama, A. Hubert-Ferrari, H. Brückner, A. Nakamura, and M. De Batist (2016). A systematic review of geological evidence for Holocene earthquakes and tsunamis along the Nankai-Suruga trough, Japan, *Earth Sci. Rev.* **159,** 337–357, doi: 10.1016/j.earscirev.2016.06.011.

Griffin, J. D., M. W. Stirling, and T. Wang (2020). Periodicity and clustering in the long-term earthquake record, *Geophys. Res. Lett.* **47,** e2020GL089272, doi: 10.1029/2020GL089272.

Hagiwara, Y. (1974). Probability of earthquake occurrence as obtained from a Weibull distribution analysis of crustal strain, *Tectonophysics* **23,** no. 3, 313–318, doi: 10.1016/0040-1951(74)90030-4.

Kempf, P., J. Moernaut, M. Van Daele, W. Vandoorne, M. Pino, R. Urrutia, and M. Batistde (2017). Coastal lake sediments reveal 5500 years of tsunami history in south central Chile, *Quat. Sci. Rev.* **161,** 99–116, doi: 10.1016/j.quascirev.2017.02.018.

Kulkarni, R., I. Wong, J. Zachariasen, C. Goldfinger, and M. Lawrence (2013). Statistical analyses of great earthquake recurrence along the Cascadia subduction zone, *Bull. Seismol. Soc. Am.* **103,** no. 6, 3205–3221, doi: 10.1785/0120120105.

Lomnitz, C. (1970). Major earthquakes and tsunamis in Chile during the period 1535 to 1955. *Geol. Rundsch.* **59,** no. 3, 938–960, doi: 10.1007/BF02042278.

Lomnitz, C. (2004). Major earthquakes of Chile: A historical survey, 1535–1960. *Seismol. Res. Lett.* **75,** no. 3, 368–378, doi: 10.1785/gssrl.75.3.368.

Matthews, M. V., W. L. Ellsworth, and P. A. Reasenberg (2002). A Brownian model for recurrent earthquakes, *Bull. Seismol. Soc. Am.* **92,** no. 6, 2233–2250, doi: 10.1785/0120010267.

Melnick, D., M. Moreno, J. Quinteros, J. C. Baez, Z. Deng, S. Li, and O. Oncken (2017). The super-interseismic phase of the megathrust earthquake cycle in Chile, *Geophys. Res. Lett.* **44,** no. 2, 784–791, doi: 10.1002/2016GL071845.

Moernaut,, J. (2020). Time-dependent recurrence of strong earthquake shaking near plate boundaries: A lake sediment perspective, *Earth Sci. Rev.*, doi: 10.1016/j.earscirev.2020.103344.

Moernaut, J., M. Daele, K. Heirman, K. Fontijn, M. Strasser, M. Pino, R. Urrutia, and M. Batist (2014). Lacustrine turbidites as a tool for quantitative earthquake reconstruction: New evidence for a variable rupture mode in south central Chile, *J Geophys Res.* **119,** no. 3, 1607–1633, doi: 10.1002/2013JB010738.

Moernaut, J., M. Daelevan, K. Fontijn, K. Heirman, P. Kempf, M. Pino, G. Valdebenito, R. Urrutia, M. Strasser, and M. De Batist (2018). Larger earthquakes recur more periodically: New insights in the megathrust earthquake cycle from lacustrine turbidite records in south-central Chile, *Earth Planet. Sci. Lett.* **481,** 9–19, doi: 10.1016/j.epsl.2017.10.016.

Moreno, M., S. Li, D. Melnick, J. R. Bedford, J. C. Baez, M. Motagh, S. Metzger, S. Vajedian, C. Sippl, B. D. Gutknecht, E. Contreras-Reyes, Z. Deng, A. Tassara, and O. Oncken (2018). Chilean megathrust earthquake recurrence linked to frictional contrast at depth, *Nat. Geosci.* **11,** no. 4, 285–290, doi: 10.1038/s41561-018-0089-5.

Nelson, A. R., C. B. DuRoss, R. C. Witter, H. M. Kelsey, S. E. Engelhart, S. A. Mahan, H. J. Gray, A. D. Hawkes, B. P. Horton, and J. S. Padgett (2021). A maximum rupture model for the central and southern Cascadia subduction zone—reassessing ages for coastal evidence of megathrust earthquakes and tsunamis, *Quat. Sci. Rev.* **261,** 106922, doi: 10.1016/j.quascirev.2021.106922.

Nishenko, S. P., and R. Buland (1987). A generic recurrence interval distribution for earthquake forecasting, *Bull. Seismol. Soc. Am.* **77,** no. 4, 1382–1399.

Pasari, S. (2019). Inverse Gaussian versus lognormal distribution in earthquake forecasting: Keys and clues, *J. Seismol.* **23,** no. 3, 537–559, doi: 10.1007/s10950-019-09822-5.

Pasari, S., and O. Dikshit (2014). Impact of three-parameter weibull models in probabilistic assessment of earthquake hazards, *Pure Appl. Geophys.* **171,** no. 7, 1251–1281, doi: 10.1007/s00024-013-0704-8.

Pasari, S., and O. Dikshit (2015). Earthquake interevent time distribution in Kachchh, northwestern India, *Earth Planets Space* **67,** no. 1, 129, doi: 10.1186/s40623-015-0295-y.

Peruzza, L., B. Pace, and F. Cavallini (2010). Error propagation in time-dependent probability of occurrence for characteristic earthquakes in Italy, *J. Seismol.* **14,** no. 1, 119–141, doi: 10.1007/s10950-008-9131-1.

Philibosian, B., and A. Meltzner (2020). Segmentation and supercycles: A catalog of earthquake rupture patterns from the Sumatran Sunda megathrust and other well-studied faults worldwide, *Quat. Sci. Rev.* **241,** doi: 10.1016/j.quascirev.2020.106390.

Rhoades, D. A., and R. J. Van Dissenvan (2003). Estimates of the time-varying hazard of rupture of the Alpine fault, New Zealand, allowing for uncertainties, *N. Z. J. Geol. Geophys.* **46,** no. 4, 479–488, doi: 10.1080/00288306.2003.9515023.

Rikitake, T. (1974). Probability of earthquake occurrence as estimated from crustal strain, *Tectonophysics* **23,** no. 3, 299–312, doi: 10.1016/0040-1951(74)90029-8.

Strasser, M., K. Monecke, M. Schnellmann, and F. S. Anselmetti (2013). Lake sediments as natural seismographs: A compiled record of late Quaternary earthquakes in central Switzerland and its implication for Alpine deformation, *Sedimentology* **60,** 319–341, doi: 10.1111/sed.12003.

Walton, M. A. L., L. M. Staisch, T. Dura, J. K. Pearl, B. Sherrod, J. Gomberg, S. Engelhart, A. Tréhu, J. Watt, J. Perkins, *et al.* (2021). Toward an integrative geological and geophysical view of Cascadia subduction zone earthquakes, *Annu. Rev. Earth Planet. Sci.* **49,** no. 1, 367–398, doi: 10.1146/annurev-earth-071620-065605.

Williams, R. T., J. R. Davis, and L. B. Goodwin (2019). Do large earthquakes occur at regular intervals through time? A perspective from the geologic record, *Geophys. Res. Lett.* **46,** no. 14, 8074–8081, doi: 10.1029/2019GL083291.

Zöller, G. (2018). A statistical model for earthquake recurrence based on the assimilation of paleoseismicity, historic seismicity, and instrumental seismicity, *J. Geophys. Res.* **123,** no. 6, 4906–4921, doi: 10.1029/2017JB015099.

Manuscript received 11 February 2021
Published online 10 November 2021